Research on On-line Monitoring Technology of Contact Temperature of GIS disconnector

Yucheng Jiang [1, a], Yiping Ma[1, b] and Zhengyong Wang[1, c]

[1]Ningbo Electric Power Design Institute Co., Ltd., Ningbo 315000, Zhejiang Province, China;

[a]nbdlsjy@163.com, [b]51101204@163.com, [c]wzy_330@163.com

Abstract

The on-line temperature monitoring of GIS disconnector is very important for the stable operation of power equipment. The sensitized and encapsulated Fiber Bragg Grating (FBG) sensor is installed on the surface of the outer shell of GIS equipment through the gasket between turns. After reflecting by the narrow band grating filter, the light wavelength is demodulated and fitted. The measured temperature is converted by the Wavelength-temperature relationship, and then the outer shell temperature and the ring of the extreme learning machine algorithm are used. The ambient temperature is used to deduce the contact temperature. The online temperature measurement method is simple and effective, and does not need to destroy the structure of existing GIS equipment, so it has good application prospects.

Keywords

GIS disconnector; Contact temperature; Fiber Bragg Grating Temperature Sensor; The Extreme Learning Machine Algorithm.

1. Introduction

With the vigorous development of China's power industry and the increasing demand, Gas Insulated Switch-gear (GIS) has been widely used in domestic and foreign power systems because of its strong interruption ability, low failure rate, easy installation and maintenance, and small space occupation. However, while GIS equipment has the advantages mentioned above, the problems of conductor loss and heating are becoming increasingly prominent due to its tight sealing, small volume, large current and other structural and operating conditions. Especially when the contact of GIS equipment is poor, due to the contact resistance becomes large, the overheating phenomenon will occur when the load current flows. Overheating of contacts and busbars will cause insulation aging and even breakdown, which will lead to short circuit and serious accidents, resulting in huge economic losses. According to incomplete statistics, many power companies at home and abroad have adopted GIS equipment, which has appeared in varying degrees the abnormal temperature phenomena and concurrent accidents caused by aging insulation or poor contact of components such as enclosed busbars, disconnectors, cable heads and so on. Therefore, it is very important for the safe and reliable operation of GIS to realize on-line monitoring of the temperature of GIS equipment and to find and eliminate the hidden danger of thermal failure in advance.

At present, there are three main measures to prevent contact overheating of GIS equipment in the field: manual observation of contact surface color, periodic measurement of circuit resistance and periodic temperature monitoring of fixed monitoring points using infrared imager. There are some shortcomings in these methods: the first two measures need to be checked and repaired by power failure of GIS equipment. In the third measure, the resolution and accuracy of the infrared imaging

technology are difficult to meet the requirements, and all three monitoring methods are difficult to achieve continuous measurement of the temperature of the GIS device, that is, online monitoring cannot be achieved. At present, infrared technology and grating fiber technology are mainly used to monitor the temperature of electrical equipment on-line. Among them, infrared temperature measurement method[6-9] can't disturb and destroy the temperature field and thermal balance inside the GIS equipment, but also solve the problem of high voltage isolation and strong magnetic field interference. However, it is necessary to install infrared temperature sensor through opening in the GIS shell and measure it. Accuracy is greatly affected by factors such as emissivity of metal surface and SF6 gas concentration. FBG technology, which uses optical wavelength as the monitoring quantity, has the advantages of not being affected by electromagnetic interference, good insulation performance, small size and light weight. It has been widely used in transformers, motors, switchgear cabinets, overhead transmission lines, cables and other power equipment, and its technology is relatively mature. The FBG temperature sensor is applied to the temperature monitoring of conductor contacts in GIS. It can accurately measure the temperature of conductor contacts without damaging the electric field and temperature field inside GIS. It has a wide application prospect.

In this paper, the location of sensor installation is determined, the temperature rise experiment of GIS disconnector is carried out, and the curve fitting of environment temperature, multi-point shell temperature and conductor contact temperature is carried out by using limit learning machine algorithm. This method can deduce the contact temperature of GIS through the environment temperature and multi-point shell temperature, and the calculation result is accurate. It can effectively solve the problem that the FBG temperature sensor can't directly measure the contact temperature.

2. Experimental principle

2.1 Principle of Fiber Bragg Grating Temperature Sensor

The FBG is fabricated by utilizing the photosensitivity of the fiber material to form spatial phase grating in the core of the fiber through ultraviolet light exposure. Its sensing principle is to obtain information by adjusting the central wavelength of FBG by external parameters. According to the grating theory, when the broadband continuous light passes through the FBG, the light wave matching the central wavelength of the FBG will be reflected, and the rest of the light wave will be transmitted directly through the FBG.

The relationship between the central wavelength of the FBG and the effective refractive index of the core and the modulation period of the FBG is expressed as follows:

$$\lambda_B = 2 n_{eff} \Lambda \tag{1}$$

Where λ_B the central wavelength of the FBG, n_{eff} the effective refractive index of the core and Λ the modulation period of the FBG are considered.

$$\frac{\Delta\lambda_B}{\lambda_B} = \left(\frac{1}{\Lambda}\frac{d\Lambda}{dT} + \frac{1}{n_{eff}}\frac{dn_{eff}}{dT} \right)\Delta T = (\alpha + \xi)\Delta T \tag{2}$$

$$\alpha = \frac{1}{\Lambda}\frac{d\Lambda}{dT} \tag{3}$$

$$\xi = \frac{1}{n_{eff}}\frac{d_{neff}}{dT} \tag{4}$$

Where α is the thermal expansion coefficient of bare grate and ξ is the thermal-optical coefficient of bare grate. Formula (2) shows that the effect of temperature change on the central wavelength of FBG is caused by thermal expansion and thermo-optic effect. Wavelength-temperature demodulation can be realized by detecting the change of incident wavelength and reflection wavelength of FBG. So the

temperature of the measured point can be calculated by measuring the variation of the central wavelength of the grating.

2.2 Main Composition of the System

The on-line monitoring system of contact temperature of GIS disconnector is mainly composed of GIS equipment, FBG sensor, demodulator and upper computer. A group of FBG temperature sensors are installed on the top of the outer wall of the disconnector, totaling 8 sensors, and two sensors are installed one meter away from the bottom of the GIS equipment to collect the environmental temperature. A high precision FBG signal demodulation system is installed in the main control room. Temperature and temperature rise information of 10 temperature measuring points on GIS are analyzed and early warning report is made.

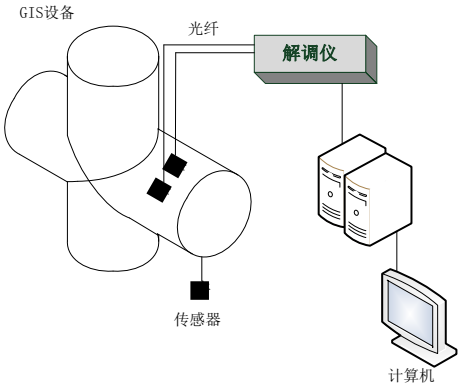

Fig. 1 System block diagram

3. Extreme Learning Machine（ELM）

3.1 Basic Ideas of ELM

ELM is a new fast learning algorithm. For single hidden layer neural networks, ELM can randomly initialize input weights and biases and obtain corresponding output weights. ELM is a fast learning algorithm for traditional neural networks proposed by Huang, especially single-hidden layer feedforward networks (SLFNs). ELM randomly initializes the input weight and hidden layer bias of SLFNs, and obtains the corresponding output weight. ELM guarantees the minimum norm of output weight, and the output weight is unique.

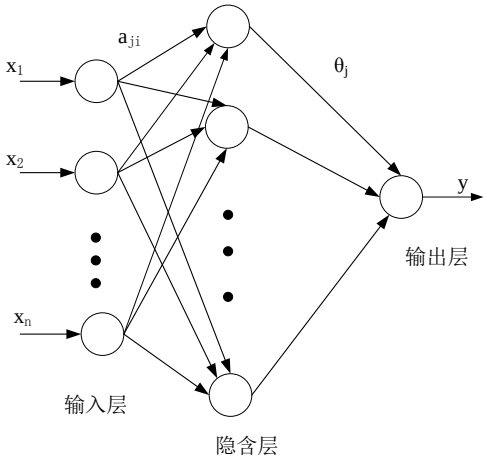

Fig. 2 ELM network structure

For N different sample $(\mathbf{x}_i, \mathbf{y}_i)$, where $\mathbf{x}_i = [x_{i1}, x_{i2}, ..., x_{in}]^T \in R^n$, $\mathbf{y}_i = [y_{i1}, y_{i2}, ..., y_{in}]^T \in R^n$ has L hidden nodes, the output of the feed-forward neural network of excitation function $G(x)$ can be expressed as

$$f(x) = \sum_{i=1}^{N} \boldsymbol{\theta}_i \bullet G(\boldsymbol{\alpha}_i \bullet \mathbf{x}_i + \boldsymbol{\beta}_i) = \mathbf{t}_i \quad \mathbf{x}_i \in \mathbf{R}^n, \boldsymbol{\beta}_i \in \mathbf{R}^n \tag{5}$$

Where $\boldsymbol{\alpha}_i = [\alpha_{i1}, \alpha_{i2}, \cdots, \alpha_{in}]^T \in \mathbf{R}^n$ is the input weight, $\boldsymbol{\theta}_i = [\theta_{i1}, \theta_{i2}, \cdots, \theta_{in}]^T \in \mathbf{R}^n$ is the output weight, $\boldsymbol{\beta}_i$ is the bias of i hidden layer unit, $\boldsymbol{\alpha}_i \bullet \mathbf{x}_i$ is the inner product of vector $\boldsymbol{\alpha}_i$ and vector $\mathbf{x}_i$, G is the excitation function of the hidden layer. Sigmoid function is used as the excitation function.

If the feedforward neural network with L hidden nodes approximates N samples with zero error and $\sum \|\mathbf{t}_i - \mathbf{y}_i\| = 0$, then there exists $\boldsymbol{\alpha}_i$、$\boldsymbol{\theta}_i$、$\boldsymbol{\beta}_i$ such that

$$f(x) = \sum_{i=1}^{N} \boldsymbol{\theta}_i \bullet G(\boldsymbol{\alpha}_i \bullet \mathbf{x}_i + \boldsymbol{\beta}_i) = \mathbf{y}_i, i = 1, 2, \cdots, L. \tag{6}$$

The matrix is expressed as

$$\mathbf{H}\boldsymbol{\theta} = \mathbf{Y}. \tag{7}$$

Where $\mathbf{H}$ is the output matrix of the hidden layer of the network, and $\mathbf{Y}$ is the expected output matrix.

If the input weights and hidden layer biases of feedforward neural networks are generated randomly, the unique solution can be obtained by Moore-penrose generalized inverse calculation. Huang has proved that the norm of the solution $\boldsymbol{\theta}$ obtained is the smallest and the solution is unique.

$$\hat{\boldsymbol{\theta}} = \mathbf{H} + \mathbf{Y}. \tag{8}$$

Where $\mathbf{H}^+$ is Moore-penrose generalized inverse of matrix $\mathbf{H}$.

Finding the output weight matrix becomes the problem of finding the least squares solution. Only the least squares solution of the input weight is required to complete the training of the neural network.

3.2 The ELM Learning Algorithms

From the previous analysis, we can know that ELM can generate $\boldsymbol{\alpha}$ and $\boldsymbol{\beta}$ randomly before training. $\boldsymbol{\theta}$ can be calculated by determining the number of neurons in the hidden layer and the activation function of the hidden layer (infinitely differentiable). So we can get the expectations we need. The basic steps are as follows:

Step 1 Input training set data $(x_1, x_2, \cdots, x_n)$, that is, the shell temperature and environment temperature of GIS disconnector equipment.

Step 2 Computer Random Determination of Input Weight α and Bias Vector β.

Step 3 To determine the number of hidden layers L and activation function $G(x)$, sig function, $\sin$ function and $\mathrm{hardlim}$ function are usually chosen by default.

Step 4 The output matrix $\mathbf{H}$ of hidden layer can be obtained from formula $\mathbf{H} = \sum_{i=1}^{N} \sum_{j=1}^{L} G(\boldsymbol{\alpha}_{ij} \bullet \mathbf{x}_i + \boldsymbol{\beta}_i)$.

Step 5 Through the output data y of the training set, that is the actual temperature of the contact, the optimal output weight $\boldsymbol{\theta}$ is obtained by from formula 9, and the predicted value is obtained from formula 7.

The ELM algorithm for temperature mapping of conductor contacts in GIS consists of input layer, hidden layer and output layer. The input variables $\mathbf{x}$ are top temperature, side temperature, bottom temperature and environment temperature of GIS equipment shell; the output variables $\mathbf{y}$ are

conductor contact temperature of GIS equipment. 95 groups of data obtained from the experiment were taken as learning samples, and 15 groups were randomly selected as testing samples. Among them, too many or too few neurons in the hidden layer will lead to the performance degradation of the network. When the training sample is close to two-thirds, the prediction accuracy is higher and the change is gentle. In the process of eigenvalue selection and model generation, in order to improve the performance of network prediction as much as possible, two-thirds of the samples are taken as the center, five points are selected before and after each, and a total of 11 test points are selected to select the best hidden layer. The target mean square error is 0.1. Through training and comparison, when the number of hidden layer nodes is 61, the error caused is the smallest, and its mean square error is 0.0888. The prediction effect is accurate. The predicted values of the high-rate algorithm are compared with the test samples as follows.

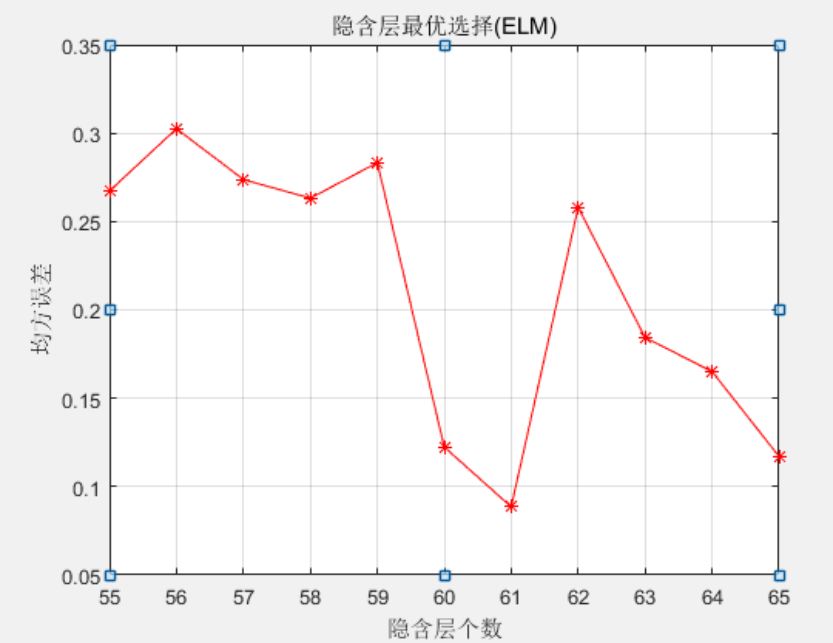

Fig.3 The relationship between the number of neurons and the performance of ELM networks

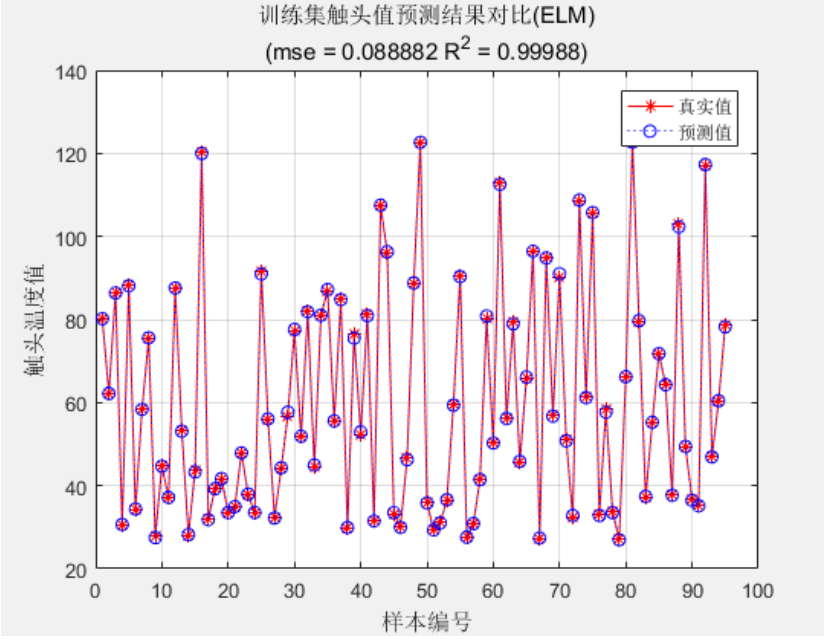

Fig. 4 Comparison of the predicted results of contact temperature in training set

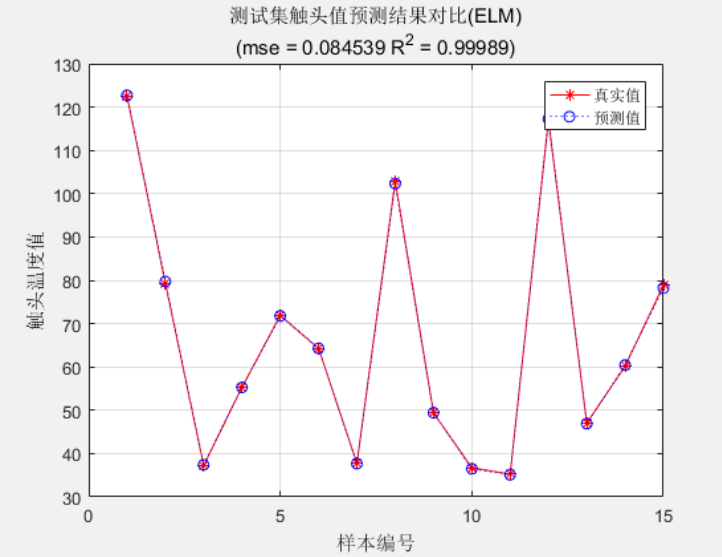

Fig. 5 Comparison of Predicted Contact Temperature Value of Test Set

The errors of training set and test set are shown in Figures 6 and 7

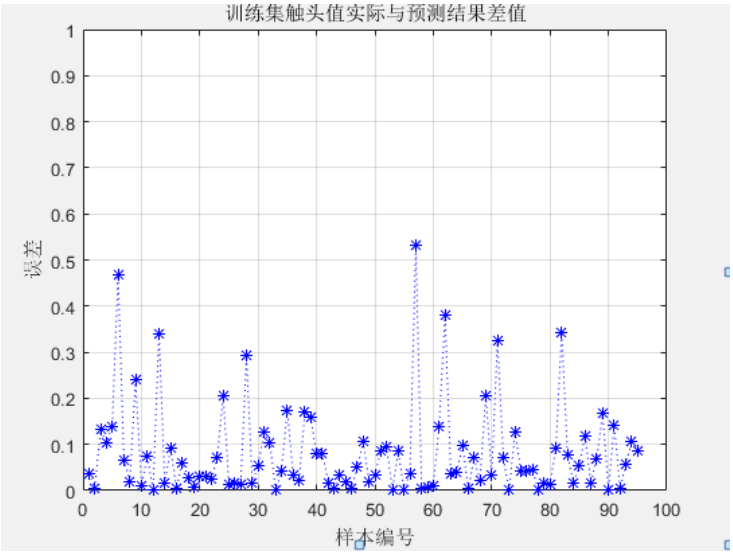

Fig. 6 Training set error

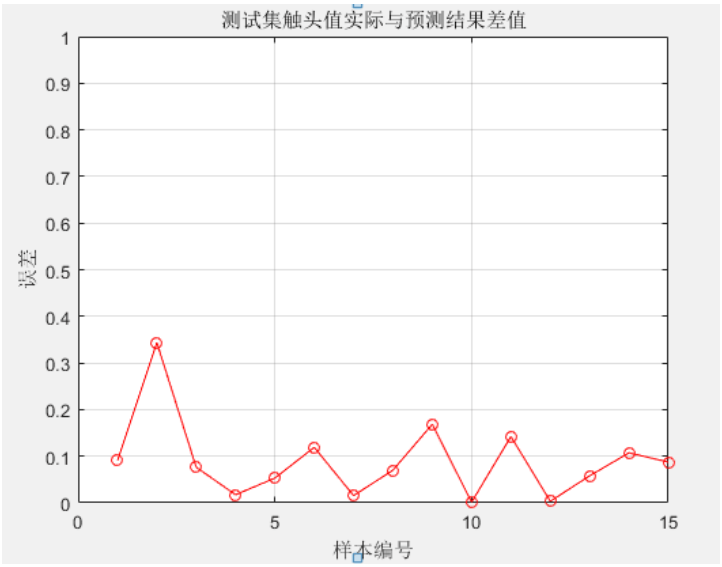

Figure 7 Test set error

The actual and predicted values of the contact temperature in the test set are shown in table 1.

Table 1 Comparisons between test samples and algorithm predictions

measured value /℃	Contact temperature predicted value /℃	relative error（%）
35.24	35.12	0.34
36.70	36.47	0.43
37.24	37.41	0.46
37.74	37.67	0.18
47.05	46.91	0.30
49.37	49.42	0.11
55.30	55.27	0.05
60.16	60.44	0.47
64.25	64.29	0.06
71.89	71.78	0.15
78.85	78.21	0.19
79.36	79.72	0.47
102.86	102.31	0.05
116.86	117.30	0.38
122.56	122.70	0.11

4. Conclusion

In view of the difficulty that FBG temperature sensor can not directly measure the temperature of conductor contact, this paper presents a method of indirectly calculating the temperature of conductor contact by using FBG temperature sensor to measure ambient temperature and multi-point shell temperature. Considering that the temperature is mainly distributed on the shell of GIS equipment, the optimum position of sensor installation is determined. A limit learning machine algorithm is proposed to calculate the contact temperature through environmental temperature and multi-point shell temperature. The calculated results are more accurate than the measured data. This method is simple, effective and fast. It does not need to destroy the existing structure of GIS equipment and has a good prospect.

References

[1] Cong H, Xing J, Li Q, et al. Infrared online temperature monitoring technology for shielded GIS contacts[J]. Electric Power Automation Equipment, 2014, 34(9):148-153.

[2] Tang L.J: Design of The Temperature Monitoring Device of The Isolated Switch Contact[D]. Harbin: Northeast Agricultural University,2016.

[3] Zhong-Xiang Li, Jian-Cheng S. On-line Temperature Measurement System for Contacts in HV Switchgear[J]. High Voltage Apparatus, 2009 ,45 (2):11-13

[4] Zu-Rong S, Xiao-Yang Li, Yi-Xuan Li, et al. Research on the Application of Optical Fiber Sensing Technology in the Nuclear Power Plant Safety Monitoring[J]. Journal of Quantum Optics, 2017 ,23(3) :297-304.

[5] X.Z, Jing X.C, Cheng D.P, et al. Application of fiber Bragg grating to temperature on-line monitoring of GIS busbar[J]. Engineering Journal of Wuhan University, ,2012 ,45 (5) :658-661.

[6] Chen R.G, Feng X.Y, Gu Chao, et al. Application of Infrared Thermometry Technology for the Fault Diagnosis in GIS[J]. High Voltage Apparatus, 2015 ,51(9) :190-194.

[7] Chen Q, Li Q.M, Cong H.X, et al. On-Line Temperature Monitoring for GIS Disconnecting Switch Contacts Based on Multipoint-Distributed Fiber Bragg Grating[J]. Transactions of China Electrotechnical Society, 2015, 30(12):298-306.
[8] Liu X.Y, Zeng J, Guo X.H, et al. The Integrated Monitoring Method of Optical Fiber Gas Pressure and Temperature Based on Reflection Spectrum Characteristic Identification[J]. Spectroscopy and Spectral Analysis, 2017 ,37 (9) :2838-2843.
[9] Wang E, Zhao Z.G, CAO Min Multi Point Temperature Monitoring of Oil Immersed Transformer Based on Fiber Bragg Grating [J]. High Voltage Engineering
[10] Cong H, Li Q, Qi B, et al. Online GIS switch contact temperature monitoring based on IR sensing[J]. Electric Power Automation Equipment, 2014,34(3):144-148.
[11] Wang Yan, Zhao Kai, Liu J.P. Optical Fiber Bragg Grating Temperature Monitoring Based on Volume Phase Grating Dispersion Demodulation[J]. Laser & Optoelectronics Progress, 2016 (10) :113-118.
[12] WU Xiaowen, SHU Naiqiu, LI Hongtao, JIN Xiangchao, XIE Zhiyang. Online temperature monitoring system based on FBG for GIS bus[J], Electric Power Automation Equipment, 2013,33(4):155-160.
[13] Li Rui, Wang B.Q, Wang X.Q. Research progress on temperature monitoring of GIS bus[J]. High Voltage Apparatus, 2012, 48(11): 130-138.
[14] Sun G.X, Guan X.Y, Shu N.Q, et al. GIS Conductor Temperature Inspection Method and Device Based on Fiber Bragg Grating[J], Transactions of China Electrotechnical Society, 2015, 30(8):316-321.
[15] Zhao D.Z, Shu N.Q, Zhang Z.L, et al. On-line temperature monitoring system of contactor in GIS based on FBG sensor network[J]. Engineering Journal of Wuhan University, 2011, 44(4): 538-541.
[16] Zhong W.Q, Sun J.W. Application of ELM in prediction of coal spontaneous Combustion in caving zone[J]. Journal of Liaoning Technical University（Natural Science）,2016,35(6):581-585.
[17] Wang J, Chang Q.K, Peng J.Z. The Optimization of the Extreme Learning Machine and Fitting Analysis[J]. Journal of Zhengzhou University, 2016,37(2):20-24.
[18] Zhao Z.Y, Li Y.X, Yu F,Yi Y.F Improved deep learning algorithm based on extreme learning machine[J]. Computer Engineering and Design,2015,36(4): 1022-1026.
[19] Huang GB, Zhou H, Ding X, et al. Extreme learning machine for regression and multiclass classification[J]. IEEE Transactions on Systems, Man, and Cybernetics,2012,42(2):513-529.
[20] Xu J.X, Yue M.Q. Aeroengine performance prognosis based on feature selection and extreme learning machine[J]. Journal of Civil Aviation University of China, 2016 ,34(1):19-23.